ELSEVIER

Mechanics of Materials 28 (1998) 207–225

MECHANICS OF MATERIALS

Generalized shape optimization of three-dimensional structures using materials with optimum microstructures

Jørgen Bay Jacobsen, Niels Olhoff *, Erik Rønholt

Institute of Mechanical Engineering, Aalborg University, 9220 Aalborg, Denmark

Received 19 November 1996; revised 3 September 1997

Abstract

This paper deals with generalized shape optimization of linearly elastic, three-dimensional continuum structures, i.e. we consider the problem of determining the structural topology (or layout) such that the shape of external as well as internal boundaries and the number of inner holes are optimized simultaneously. For prescribed static loading and given boundary conditions, the optimum solution is sought from the condition of maximum integral stiffness (minimum elastic compliance) subject to a specified amount of structural material within a given three-dimensional design domain. This generalized shape optimization problem requires relaxation which leads to the introduction of microstructures. A class of optimum three-dimensional microstructures and explicit analytical expressions for their optimum effective stiffness properties have been developed by Gibiansky and Cherkaev (1987) [Gibiansky, L.V., Cherkaev, A.V., 1987. Microstructures of composites of extremal rigidity and exact estimates of provided energy density (in Russian). Report (1987) No. 1155. A.F. Ioffe Physical-Technical Institute, Academy of Sciences of the USSR, Leningrad. English translation in: Kohn, R.V., Cherkaev, A.V. (Eds.), Topics in the Mathematical Modelling of Composite Materials. Birkhaüser, New York. 1997]. The present paper gives a brief account of the results in Gibiansky and Cherkaev (1987) which will be utilized for our microlevel problem analysis. It is a characteristic feature that the use of optimum microstructures renders the global problem convex if an appropriate parametrization is applied. Hereby local optima can be avoided and we can construct a simple gradient based numerical method of mathematical programming for solution of the complete optimization problem. Illustrative examples of optimum layout and topology designs of three-dimensional structures are presented at the end of the paper.

Keywords: Optimum structural design; Three-dimensional layout and topology optimization; Optimum material microstructures; Homogenization; Mathematical programming

1. Introduction

Topology optimization of continuum structures was introduced in the literature by the landmark paper by Bendsøe and Kikuchi (1988) (see also Bendsøe, 1989) and has since been an extremely active area of research. Topology optimization is decisive for the cost-efficiency of a structure and is most valuable as a preprocessing

* Corresponding author.

0167-6636/98/$19.00
PII: S0167-6636(97)00056-2

tool for refined shape or sizing optimization (Olhoff et al. (1991)). An exhaustive account of the current status of the field has recently been published in a monograph (Bendsøe, 1995) by Bendsøe which witnesses that up to now, layout and topology optimization of continuum structures have been almost exclusively reserved for two-dimensional problems. The present paper may be considered as a generalization of topology optimization to three-dimensional structures (see also the recent papers Cherkaev and Palais (1996) and Allaire et al. (1996)). The papers (Bendsøe and Kikuchi, 1988; Bendsøe, 1989) as well as studies of similar two-dimensional problems published earlier by Lurie et al. (1982a,b), Cheng and Olhoff (1981, 1982), Olhoff et al. (1981) and Kohn and Strang (1982), have shown that topology optimization problems are generally not well-posed unless the formulation of the problem is relaxed by introducing composites with perforated, periodic microstructures.

Gibiansky and Cherkaev (1987) and later Allaire (1994) derived the optimum effective properties of such microstructures in explicit analytical form which is highly desirable for practical implementation. As outlined in Section 2, these authors derived the minimum complementary energy density for the class of matrix layered composites (MLC) of any rank and applied this as an upper bound on the energy density. At the same time, as will be discussed in Section 3, the authors applied the theory of quasiconvexification to construct a lower bound on the complementary energy density of a composite which is valid for composites of any microstructure. The optimum composites are characterized by having a complementary energy density which lies between these two bounds and it is shown in Gibiansky and Cherkaev (1987) that for the limiting case of perforated composites, these bounds coalesce and yield analytical expressions for the optimum properties of perforated rank three MLCs. These results are summarized at the end of Section 3 and briefly discussed in Section 4.

On the basis of these analytical results (Gibiansky and Cherkaev, 1987) for optimization at the microstructural level, the global problem of maximizing the integral structural stiffness is easily established. Maximization of the structural stiffness is equivalent to minimization of the total elastic energy and the sensitivity analysis of the total elastic energy and material volume of the structure can be carried out analytically. Thus, an iterative numerical procedure based on finite element analysis, sensitivity analysis and mathematical programming has been developed for solution of the complete three-dimensional topology optimization problem. This procedure is presented in Section 5.

Section 6 presents several examples of generalized shape optimization of three-dimensional structures and contains a brief summary discussion of the new method.

2. Formulation of the microstructure problem

The analysis in this paper and the subsequent section follows Gibiansky and Cherkaev (1987) in establishing analytical expressions for the complementary energy density E and elastic properties of the microstructure that is optimum subject to a given three-dimensional state of stress in a given point of the structure.

This will be achieved by construction of an upper and a lower bound $E_l \leq E \leq E_u$ for the complementary elastic energy density E of the optimum microstructure. The upper bound E_u will be established in this section by minimization of the complementary energy density of a bi-material MLC of any rank and the lower bound E_l (which is valid for any bi-material microstructure) will be developed in Section 3 by means of quasiconvexification. The optimum characteristics of the microstructure for the purpose of topology optimization are derived subsequently in Section 3 by utilizing the fact (Gibiansky and Cherkaev, 1987) that in the limit where the compliance of one of the two materials tends to infinity in order to mimic void, the abovementioned bounds coalesce with E so that $E_l = E = E_u$ and from this follow the desired analytical results.

Now, following Gibiansky and Cherkaev (1987) and referring to Fig. 1, we consider a three-dimensional layered composite microstructure of rank three. As we consider a single case of loading, the layers are mutually orthogonal, and the composite is made of two isotropic, linear elastic materials with 6×6 dimensional

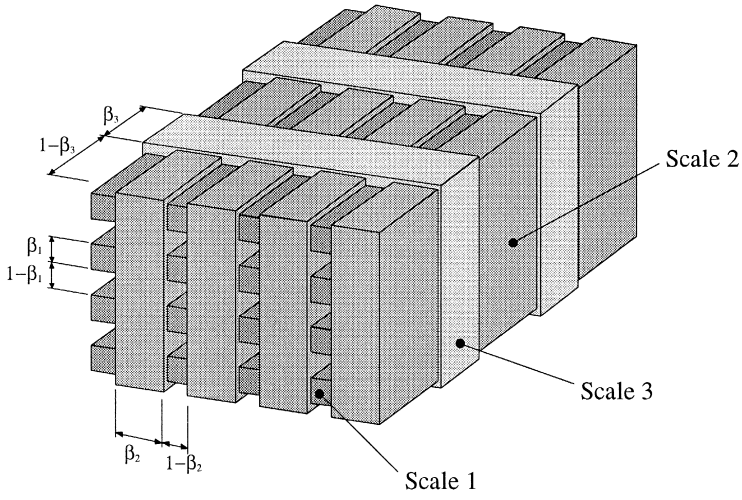

Fig. 1. Model of a spatial rank three laminate where β_i denotes the ith length scale.

compliance matrices denoted by $\mathbf{C}_1$ and $\mathbf{C}_2$, respectively. The compliance matrices which are the inverted elasticity matrices are given by

$$\mathbf{C}(\kappa,\mu)=\begin{bmatrix} \frac{3\kappa+\mu}{9\kappa\mu} & \frac{2\mu-3\kappa}{18\kappa\mu} & \frac{2\mu-3\kappa}{18\kappa\mu} & 0 & 0 & 0 \\ \frac{2\mu-3\kappa}{18\kappa\mu} & \frac{3\kappa+\mu}{9\kappa\mu} & \frac{2\mu-3\kappa}{18\kappa\mu} & 0 & 0 & 0 \\ \frac{2\mu-3\kappa}{18\kappa\mu} & \frac{2\mu-3\kappa}{18\kappa\mu} & \frac{3\kappa+\mu}{9\kappa\mu} & 0 & 0 & 0 \\ 0 & 0 & 0 & \frac{1}{2\mu} & 0 & 0 \\ 0 & 0 & 0 & 0 & \frac{1}{2\mu} & 0 \\ 0 & 0 & 0 & 0 & 0 & \frac{1}{2\mu} \end{bmatrix} \tag{1}$$

where κ and μ are the bulk and shear moduli, respectively, and indices for the two materials have been omitted. The effective elastic properties of the resulting anisotropic material depend on the material properties of the two constituents given by $\mathbf{C}_1$ and $\mathbf{C}_2$, the normals $\boldsymbol{n}$ to the material interfaces and the volume fractions m_1 and m_2 $(m_2 = 1 - m_1)$ of the two materials. Furthermore, knowledge on how the material is distributed between the different layers is required.

The length scales (Fig. 1) describe the relative thickness of each layer which yields the following relation between volume density ρ and length scales for a rank n material

$$\rho_n = \beta_n + (1-\beta_n)\,\rho_{n-1} \tag{2}$$

where, in the case of a rank three material,

$$\beta_1 = m_1\alpha_1, \qquad \beta_2 = \frac{m_1\alpha_2}{1 - m_1\alpha_1}, \qquad \beta_3 = \frac{m_1\alpha_3}{1 - m_1(1-\alpha_3)} \tag{3}$$

The introduced parameter α_i denotes the spatial thickness of layer i which means that it can be considered as a volume density for the layer. By introducing this parameter the basic idea is to equalize the stresses in the different directions by varying the spatial thickness of each layer. As a function of this parameter the expression for the optimum compliance tensor $\mathbf{C}_M$, for a rank n MLC is given by

$$\mathbf{C}_M = \mathbf{C}_1 + \mathbf{Q}^{-1} \tag{4}$$

where

$$\mathbf{Q} = \frac{1}{m_2}(\mathbf{C}_2 - \mathbf{C}_1)^{-1} + \frac{m_1}{m_2}\sum_{i=1}^{n}\alpha_i\mathbf{N}_i, \qquad \mathbf{N}_i = \mathbf{N}(\boldsymbol{n}_i) = \mathbf{p}_i\left(\mathbf{p}_i^{\mathrm{T}}\mathbf{C}_1\mathbf{p}_i\right)^{-1}\mathbf{p}_i^{\mathrm{T}}, \qquad \sum_{i=1}^{n}\alpha_i = 1, \quad \alpha_i \geq 0 \tag{5}$$

The projection matrix $\mathbf{p}_i$ controls discontinuous stress components across the material interfaces and $\boldsymbol{n}_i$ is the normal to the ith layer. Inserting this result in the expression for the complementary energy density, we get the following equation for a minimum value of the upper bound energy density E_{u} with respect to the variables α_i and $\boldsymbol{n}_i$

$$E_{\mathrm{u}} = \boldsymbol{\sigma}^{\mathrm{T}}\mathbf{C}_1\boldsymbol{\sigma} + \min_{\alpha_i,\boldsymbol{n}_i}\boldsymbol{\sigma}^{\mathrm{T}}\mathbf{Q}^{-1}\boldsymbol{\sigma} \tag{6}$$

where $\boldsymbol{\sigma}$ is a 6×1 vector of stress components defined as

$$\boldsymbol{\sigma} = (\,\sigma_{11}\ \sigma_{22}\ \sigma_{33}\ \sigma_{12}\ \sigma_{13}\ \sigma_{23}\,)^{\mathrm{T}}$$

Assuming that we are dealing with a rank three material that is oriented along the principal stress directions, we can write

$$\sum_{i=1}^{3}\alpha_i\mathbf{N}_i = \frac{2\mu_1}{3\kappa_1 + 4\mu_1}\begin{bmatrix}\mathbf{B}_1 & \mathbf{0}\\ \mathbf{0} & \mathbf{B}_2\end{bmatrix} \tag{7}$$

where the matrices $\mathbf{B}_1$ and $\mathbf{B}_2$ are given by

$$\mathbf{B}_1 = \begin{bmatrix} 2(3\kappa_1+\mu_1)(\alpha_2+\alpha_3) & (3\kappa_1-2\mu_1)\alpha_3 & (3\kappa_1-2\mu_1)\alpha_2 \\ (3\kappa_1-2\mu_1)\alpha_3 & 2(3\kappa_1+\mu_1)(\alpha_1+\alpha_3) & (3\kappa_1-2\mu_1)\alpha_1 \\ (3\kappa_1-2\mu_1)\alpha_2 & (3\kappa_1-2\mu_1)\alpha_1 & 2(3\kappa_1+\mu_1)(\alpha_1+\alpha_2) \end{bmatrix},$$

$$\mathbf{B}_2 = \begin{bmatrix} (3\kappa_1+4\mu_1)\alpha_3 & 0 & 0 \\ 0 & (3\kappa_1+4\mu_1)\alpha_2 & 0 \\ 0 & 0 & (3\kappa_1+4\mu_1)\alpha_1 \end{bmatrix}, \tag{8}$$

respectively.

Expanding to the global structural level, we can formulate the total elastic energy minimization problem, incorporating optimum microstructures, and subject to a given upper bound V_{fixed} on the total amount of material, as

$$\begin{aligned}
\min_{\alpha_i^k,\theta_k,\rho_k} \quad & \int_\Omega \left(\boldsymbol{\sigma}^{\mathrm{T}} \mathbf{C}_1 \boldsymbol{\sigma} + \boldsymbol{\sigma}^{\mathrm{T}} \mathbf{Q}^{-1} \boldsymbol{\sigma} \right) \mathrm{d}\Omega \quad k = 1, \ldots, N \\
\text{subject to} \quad & \nabla \boldsymbol{\sigma} = 0, \\
& \sum_{i=1}^{3} \alpha_i^k = 1, \; 0 \le \alpha_i \le 1, \qquad k = 1, \ldots, N, \\
& \sum_{k=1}^{N} \rho_k v_k \le V_{\text{fixed}}, \\
& 0 \le \rho_k \le 1, \qquad k = 1, \ldots, N
\end{aligned} \tag{9}$$

where α_i^k, $i = 1, 2, 3$ and θ_k are variables describing the layout and orientation of the microstructure in the kth finite element, ρ_k is the volume fraction of material within the same element and N is the total number of finite elements. Here, the equilibrium equation $\nabla \boldsymbol{\sigma} = 0$ will be satisfied through finite element analysis of the structure and the minimization with respect to θ_k will be performed by orienting the microstructure along the principal stresses in each finite element. The minimization with respect to α_i^k can be done analytically via explicit analytical expressions for the optimum values of α_i to be derived in Section 3 and minimization with respect to ρ_k can be carried out by means of mathematical programming as described in Section 5.

3. Optimum material properties

Referring to the initial discussion in Section 2, the expression for maximum value of the lower bound E_1 for the complementary energy density E of any microstructure made with volume fractions m_1 and $m_2 = (1 - m_1)$ of two elastic materials with compliance matrices $\mathbf{C}_1$ and $\mathbf{C}_2$, is given by (Gibiansky and Cherkaev, 1987)

$$E_1 = \max_{a_j} \boldsymbol{\sigma}^{\mathrm{T}} \boldsymbol{\beta}\left(\mathbf{C}_1, \mathbf{C}_2, \boldsymbol{\Phi}(a_j)\right) \boldsymbol{\sigma} \tag{10}$$

with the compliance matrix $\boldsymbol{\beta}(\mathbf{C}_1, \mathbf{C}_2, \boldsymbol{\Phi}(a_j))$ defined by

$$\boldsymbol{\beta} = \left[\left[m_1 (\mathbf{C}_1 - \boldsymbol{\Phi})^{-1} + m_2 (\mathbf{C}_2 - \boldsymbol{\Phi})^{-1} \right]^{-1} + \boldsymbol{\Phi} \right] \tag{11}$$

where

$$\boldsymbol{\Phi} = \begin{bmatrix}
a_1^2 & -a_1 a_2 & -a_1 a_3 & 0 & 0 & 0 \\
-a_1 a_2 & a_2^2 & -a_2 a_3 & 0 & 0 & 0 \\
-a_1 a_3 & -a_2 a_3 & a_3^2 & 0 & 0 & 0 \\
0 & 0 & 0 & a_2^2 + a_3^2 & 0 & 0 \\
0 & 0 & 0 & 0 & a_1^2 + a_3^2 & 0 \\
0 & 0 & 0 & 0 & 0 & a_1^2 a_2^2
\end{bmatrix} \tag{12}$$

is the non-convex function that makes E_1 quasiconvex. Here a_j, $j=1, 2, 3$, are scalar parameters and the maximization in Eq. (10) is to be carried out with respect to these. The parameters a_1, a_2, a_3 must satisfy the constraints of positive definiteness of the matrices $\mathbf{C}_i - \boldsymbol{\Phi}(a_1, a_2, a_3)$, $i=1, 2$, which ensures positive definiteness of the compliance matrix $\boldsymbol{\beta}$, Eq. (11), and hence positive complementary energy density for all $\boldsymbol{\sigma}$ in Eq. (10).

In the case of topology optimization, where the compliant material is considered as void, the expressions for the effective properties of the microstructure simplify considerably so that the optimal properties can be expressed in explicit analytic form (Gibiansky and Cherkaev, 1987). Thus, letting $\mathbf{C}_2 \to \infty$ to mimic void, the term $(\mathbf{C}_2 - \boldsymbol{\Phi})^{-1}$ of $\boldsymbol{\beta}(\mathbf{C}_1, \mathbf{C}_2, \boldsymbol{\Phi}(a_j))$ in Eq. (11) vanishes and the following expression for E_1 is obtained

$$E_1 = \max_{a_j} \boldsymbol{\sigma}^{\mathrm{T}} \left[\left[1 + \frac{m_2}{m_1} \right] \mathbf{C}_1 - \frac{m_2}{m_1} \boldsymbol{\Phi} \right] \boldsymbol{\sigma} = \boldsymbol{\sigma}^{\mathrm{T}} \mathbf{C}_1 \boldsymbol{\sigma} + \frac{m_2}{m_1} \max_{a_j} \boldsymbol{\sigma}^{\mathrm{T}} \mathbf{G} \boldsymbol{\sigma} \tag{13}$$

where $\mathbf{G} = (\mathbf{C}_1 - \boldsymbol{\Phi})$. Since $\boldsymbol{n}_i$ are assumed oriented along the principal directions of $\boldsymbol{\sigma}$, it is only the upper 3×3 blocks of $\mathbf{C}_1$ and $\mathbf{G}$ that have an influence upon the resulting bound. The lower bound E_1 can then be formulated as

$$E_1 = \hat{\boldsymbol{\sigma}}^{\mathrm{T}} \hat{\mathbf{C}}_1 \hat{\boldsymbol{\sigma}} + \frac{m_2}{m_1} \max_{a_j} \hat{\boldsymbol{\sigma}}^{\mathrm{T}} \hat{\mathbf{G}} \hat{\boldsymbol{\sigma}} \tag{14}$$

where $\hat{\boldsymbol{\sigma}}$ indicates principal stresses and $\hat{\mathbf{G}}$ and $\hat{\mathbf{C}}_1$ indicate the upper-left 3×3 blocks of the 6×6 matrices $\mathbf{G}$ and $\mathbf{C}_1$, respectively. If a_j is chosen optimally we can write

$$E_1 = \hat{\boldsymbol{\sigma}}^{\mathrm{T}} \left[\hat{\mathbf{C}}_1 + \frac{m_2}{m_1} \hat{\mathbf{G}} \right] \hat{\boldsymbol{\sigma}} \tag{15}$$

Assuming that $\boldsymbol{\sigma}$ is oriented along the principal directions such that $\boldsymbol{\sigma}^{\mathrm{T}} = (\sigma_1, \sigma_2, \sigma_3, 0, 0, 0)$ and by defining principal stress ratios ω and η as

$$\omega = \frac{\sigma_1}{\sigma_3}, \qquad \eta = \frac{\sigma_2}{\sigma_3} \quad \text{where } \sigma_3 \geq |\sigma_2| \text{ and } \sigma_3 \geq |\sigma_1| \tag{16}$$

the optimum values of the parameters a_j can be derived in an explicit analytical form by assuming that the optimum solution lies on the edges or vertices of the design space. The expressions for the optimum parameters a_j change with changing stresses and it turns out (Gibiansky and Cherkaev, 1987) that the entire stress domain is covered by nine different sets of expressions for the optimum parameters a_j. These expressions can be used to determine the optimum values of the microstructural parameters α_i associated with the upper bound (Gibiansky and Cherkaev, 1987).

Considering the upper bound E_{u} in Eq. (6) with $\mathbf{Q}$ given in Eq. (5) and letting $\mathbf{C}_2 \to \infty$, the first term of $\mathbf{Q}$ equals zero. However, assuming that the rank three microstructure is oriented along the principal stress directions, the second term in the expression for $\mathbf{Q}$ simplifies and the following expression for E_{u} is obtained

$$E_{\mathrm{u}} = \hat{\boldsymbol{\sigma}}^{\mathrm{T}} \hat{\mathbf{C}}_1 \hat{\boldsymbol{\sigma}} + \min_{\alpha_i} \hat{\boldsymbol{\sigma}}^{\mathrm{T}} \hat{\mathbf{Q}}^{-1} \hat{\boldsymbol{\sigma}} \tag{17}$$

Provided that α_i, $i=1, 2, 3$, are chosen optimally we can write

$$E_{\mathrm{u}} = \hat{\boldsymbol{\sigma}}^{\mathrm{T}} \left[\hat{\mathbf{C}}_1 + \hat{\mathbf{Q}}^{-1} \right] \hat{\boldsymbol{\sigma}} = \hat{\boldsymbol{\sigma}}^{\mathrm{T}} \hat{\mathbf{C}}_M \hat{\boldsymbol{\sigma}} \tag{18}$$

where $\hat{\mathbf{C}}_M$ is the optimum effective compliance matrix. In Eqs. (17) and (18) the vector $\hat{\boldsymbol{\sigma}}$ and the matrices $\hat{\mathbf{C}}_1$, $\hat{\mathbf{Q}}$ and $\hat{\mathbf{C}}_M$ are all expressed in the basis $\boldsymbol{n}_i$, oriented along the principal directions of $\boldsymbol{\sigma}$. It is shown in

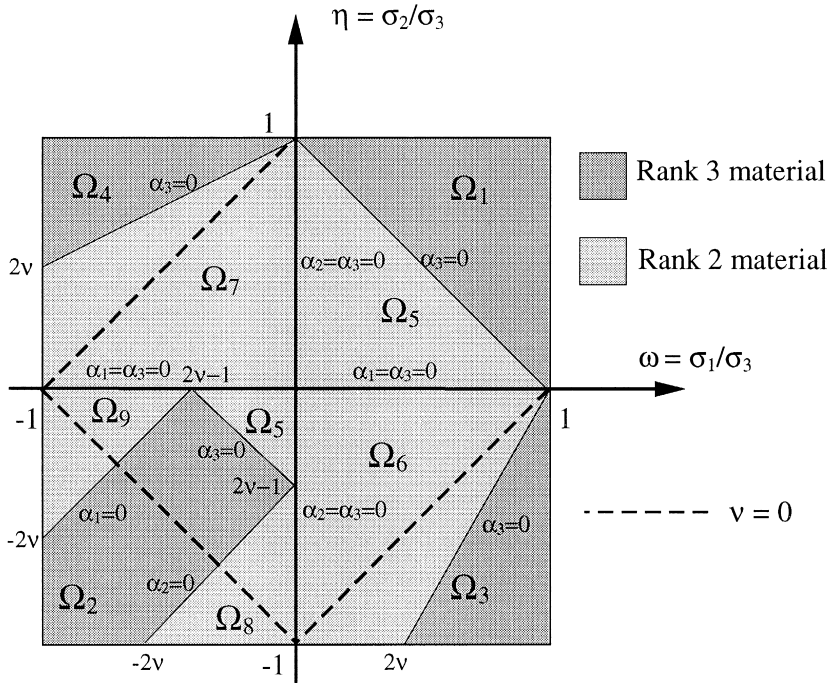

Fig. 2. The domain Ω with individual sub-domains Ω_i.

Gibiansky and Cherkaev (1987) that the two bounds E_u and E_1 coalesce for an optimum microstructure which implies that for any admissible a_j the following difference is equal to zero

$$E_u(\boldsymbol{\sigma}) - E_1(\boldsymbol{\sigma}) = \max_{a_i} \min_{\alpha_i} \boldsymbol{\sigma}^T \left(\mathbf{Q}^{-1}(\alpha_i) - \mathbf{G}(a_j) \right) \boldsymbol{\sigma} = 0 \tag{19}$$

which after some algebra (Gibiansky and Cherkaev, 1987) can be reduced to

$$\left(\hat{\mathbf{Q}}(\alpha_i) \hat{\mathbf{G}}_i - \mathbf{I} \right) \hat{\boldsymbol{\sigma}} = 0 \tag{20}$$

where $\mathbf{I}$ is the unit matrix. In order to solve this problem we first determine the eigenvalues of the 3×3 matrix $\hat{\mathbf{Q}}(\alpha_i)\hat{\mathbf{G}}_i$. It can be shown that for all matrices $\hat{\mathbf{Q}}(\alpha_i)\hat{\mathbf{G}}_i$ the corresponding eigenvalues are equal to (0, 0, 1) and the corresponding eigenvector yields a set of equations which upon solution yields the optimum α_i that satisfy Eq. (20).

The solution for α_i reveals that the relation between the principal stresses and the optimum microstructure changes for different stresses and that the entire stress domain is divided into nine sub-domains (Fig. 2) with different relations. The expressions for the individual domains are listed in Eqs. (21a), (21b), (21c), (21d), (21e), (21f), (21g), (21h) and (21i), where ν denotes Poisson's ratio.

$$\alpha_1 = \frac{1 - \omega + \eta}{1 + \omega + \eta}, \qquad \alpha_2 = \frac{1 + \omega - \eta}{1 + \omega + \eta}, \qquad \alpha_3 = \frac{\omega + \eta - 1}{1 + \omega + \eta}, \quad \text{if } \boldsymbol{\sigma} \in \Omega_1 \tag{21a}$$

$$\alpha_1 = \frac{-\omega + \eta - (1 - 2\nu)}{(1 - 2\nu)(\omega + \eta - (1 + 2\nu))}, \qquad \alpha_2 = \frac{\omega - \eta - (1 - 2\nu)}{(1 - 2\nu)(\omega + \eta - (1 + 2\nu))},$$

$$\alpha_3 = \frac{\omega + \eta + (1 - 2\nu)}{\omega + \eta - (1 + 2\nu)}, \quad \text{if } \boldsymbol{\sigma} \in \Omega_2 \tag{21b}$$

$$\alpha_1 = \frac{1-\omega-(1-2\nu)\eta}{(1-2\nu)(1+\omega-(1+2\nu)\eta)}, \qquad \alpha_2 = \frac{1+\omega+(1-2\nu)\eta}{1+\omega-(1+2\nu)\eta},$$

$$\alpha_3 = \frac{\omega-(1-2\nu)\eta-1}{(1-2\nu)(1+\omega-(1+2\nu)\eta)}, \quad \text{if } \boldsymbol{\sigma} \in \Omega_3 \tag{21c}$$

$$\alpha_1 = \frac{\eta-1-\omega(1-2\nu)}{(1-2\nu)(1-(1+2\nu)\omega+\eta)}, \qquad \alpha_2 = \frac{1-\omega(1-2\nu)-\eta}{(1-2\nu)(1-(1+2\nu)\omega+\eta)},$$

$$\alpha_3 = \frac{1+\omega(1-2\nu)+\eta}{1-(1+2\nu)\omega+\eta}, \quad \text{if } \boldsymbol{\sigma} \in \Omega_4 \tag{21d}$$

$$\alpha_1 = \frac{\eta}{\omega+\eta}, \qquad \alpha_2 = \frac{\omega}{\omega+\eta}, \qquad \alpha_3 = 0, \quad \text{if } \boldsymbol{\sigma} \in \Omega_5 \tag{21e}$$

$$\alpha_1 = -\frac{\eta}{\omega-\eta}, \qquad \alpha_2 = \frac{\omega}{\omega-\eta}, \qquad \alpha_3 = 0, \quad \text{if } \boldsymbol{\sigma} \in \Omega_6 \tag{21f}$$

$$\alpha_1 = -\frac{\eta}{\omega-\eta}, \qquad \alpha_2 = \frac{\omega}{\omega-\eta}, \qquad \alpha_3 = 0, \quad \text{if } \boldsymbol{\sigma} \in \Omega_7 \tag{21g}$$

$$\alpha_1 = \frac{1}{1-\omega}, \qquad \alpha_2 = 0, \qquad \alpha_3 = \frac{\omega}{\omega-1}, \quad \text{if } \boldsymbol{\sigma} \in \Omega_8 \tag{21h}$$

$$\alpha_1 = 0, \qquad \alpha_2 = \frac{1}{1-\eta}, \qquad \alpha_3 = -\frac{\eta}{1-\eta}, \quad \text{if } \boldsymbol{\sigma} \in \Omega_9 \tag{21i}$$

Eqs. (21a), (21b), (21c), (21d), (21e), (21f), (21g), (21h) and (21i) constitute the analytically derived solution to the local microstructure optimization problem. From Fig. 2 it is clear that if the size of all principal stresses are in the same range, the resulting microstructure is a rank three laminate, whereas the resulting microstructure is a rank two laminate if one principal stress is considerably less than the two others.

4. Parametric study of the microstructure

An extensive parametric study of the method has been performed in order to verify the derived expressions. By plotting the energy density E versus ω and η over the entire stress domain it is verified that the problem of determining the optimum microstructure is continuous (but not differentiable due to the quasiconvexity) and as the material distribution problem is relaxed, a stable convergence of the problem is ensured. With a rigorous three-dimensional method developed, it is interesting to compare the relative energy (stiffness) between the optimum microstructure and the non-relaxed material model used for isotropic materials (commonly referred to as a solid isotropic microstructure, see Rozvany et al. (1995)). A plot of the relative energy density $E_{\text{rel}} = E_{\text{iso}}/E_{\text{aniso}}$ versus the volume density ρ of material is shown in Fig. 3.

The energy density of anisotropic material is not uniquely defined because it varies with varying stresses, but if we vary the stress field within the admissible limits for a fixed volume density of material ρ, we get the

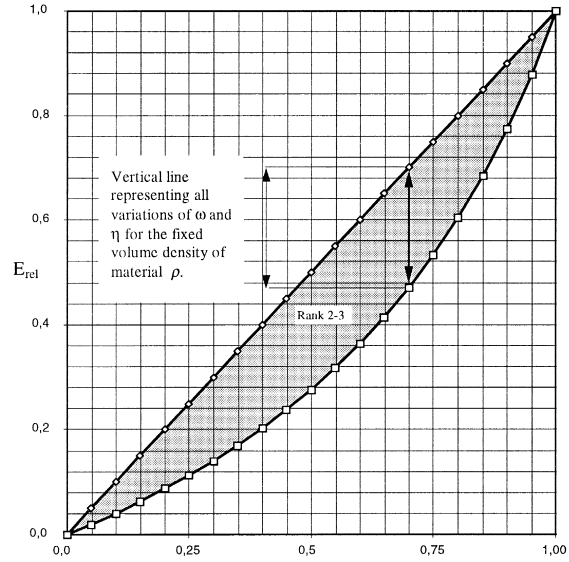

Fig. 3. Relative energy density $E_{rel} = E_{iso} / E_{aniso}$ versus the volume density ρ of material for the entire range of principal stress ratios ω and η.

results in Fig. 3. The upper limit of the grey region corresponds to a rank 1 material while the lower limit corresponds to a rank 3 material. An essential observation is that the energy density of the ranked optimum anisotropic material is always higher than (in the special case of a uniaxial stress, equal to) that of the isotropic material law, in all points but $\rho = 0$ (void) and $\rho = 1$ (solid material). This indicates that the commonly used assumption of a linear material density to stiffness relation overestimates the stiffness of a given structure if intermediate densities occur. This is in perfect agreement with results obtained by Sigmund (1994) for plane laminates.

5. Solution of the complete optimization problem

Design for maximum stiffness of statically loaded linearly elastic structures is equivalent to design for minimum compliance defined as the work done by the set of given loads against the displacements at equilibrium. This is, in turn, equivalent to minimizing the total elastic energy U at the equilibrium state of the structure. Thus we consider the material distribution problem of maximizing the integral structural stiffness subject to a given upper limit on the total volume of material in the form of minimizing the total elastic energy U at equilibrium.

We solve this problem by an iterative procedure as shown in Fig. 4. The procedure consists of a main loop for solution of the global problem of distribution of the total volume of material into local densities ρ of material and an inner loop for solution of the local problem everywhere.

Each iteration in the inner loop is initiated by a finite element analysis from which the principal stresses and their directions are calculated, and followed by (i) computing everywhere the volume densities α_i for the layers $i = 1, 2, 3$ of the local microstructure by substituting the principal stresses into Eqs. (16), (21a), (21b), (21c), (21d), (21e), (21f), (21g), (21h) and (21i) and (ii) orienting the local microstructures along the principal stress directions.

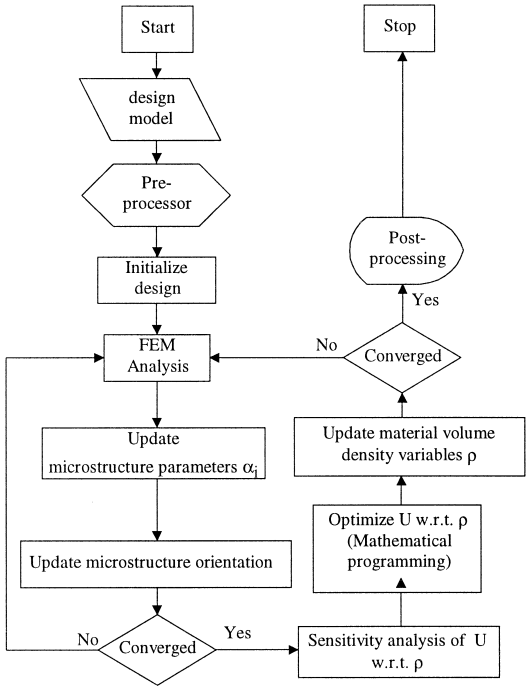

Fig. 4. Flow diagram of iterative solution procedure.

In the inner loop for the optimization of the microstructures, the local volume densities ρ of material are kept unchanged and, except for the initial finite element analysis, the loop essentially encompasses substitution into known analytical expressions.

When the iterations of the inner loop have converged, these are kept fixed and we proceed to the outer loop, see Fig. 4, which is associated with the global problem of determining a set of improved values of the local densities ρ of material with a view to minimize the total elastic strain energy U at equilibrium subject to the given limit V_{fixed} on the total volume of structural material at our disposal. Contrary to the microstructure problem, the global material distribution problem is of numerical nature and it is formulated as follows using finite element notation:

$$
\begin{aligned}
&\min_{\rho_k} && U = \frac{1}{2}\mathbf{D}^{\mathrm{T}}\mathbf{K}\mathbf{D} = \frac{1}{2}\sum_{k=1}^{N} \boldsymbol{d}_k^{\mathrm{T}}\boldsymbol{k}_k\boldsymbol{d}_k \\
&\text{subject to} && \mathbf{K}\mathbf{D} - \mathbf{R} = \mathbf{0} \\
& && \sum_{k=1}^{N} \rho_k \nu_k - V_{\text{fixed}} \le 0 \\
& && 0 \le \rho_k \le 1, \quad k = 1, \ldots, N \\
&\text{where} && \boldsymbol{k}_k = \int_{\nu_k} \mathbf{B}_k^{\mathrm{T}}\mathbf{E}_k\mathbf{B}_k \,\mathrm{d}\nu_k
\end{aligned}
\tag{22}
$$

Here, the volume densities ρ_k of material, which are assumed to be constant within each individual finite element $k = 1, \ldots, N$ are the design variables and the global stiffness matrix $\mathbf{K}$ and nodal displacement vector

D depend on these. Upper case symbols denote global level while lower case symbols denote element level. **R** is the load vector and the constraints imposed on the problem are the equilibrium condition, the global volume constraint and the volume constraint within each finite element.

The sensitivity analysis of the objective function U with respect to ρ_k can be performed analytically as follows. The change of the total elastic energy

$$U = \frac{1}{2}\mathbf{D}^{\mathrm{T}}\mathbf{K}\mathbf{D} \tag{23}$$

due to a change in any of the design variables ρ_k, $k = 1, \ldots, N$, can be expressed as

$$\frac{\partial U}{\partial \rho_k} = \frac{1}{2}\left(\mathbf{D}^{\mathrm{T}}\frac{\partial \mathbf{K}}{\partial \rho_k}\mathbf{D} + \frac{\partial \mathbf{D}^{\mathrm{T}}}{\partial \rho_k}\mathbf{K}\mathbf{D} + \mathbf{D}^{\mathrm{T}}\mathbf{K}\frac{\partial \mathbf{D}}{\partial \rho_k}\right) \tag{24}$$

where the first term arises from the change in energy due to the change in the stiffness matrix and the next terms stem from the change of the displacement field. Assuming design independent loads, the derivative of the equilibrium condition $\mathbf{K}\mathbf{D} - \mathbf{R} = \mathbf{0}$ with respect to the design variables, can be formulated as

$$\frac{\partial \mathbf{K}}{\partial \rho_k}\mathbf{D} = -\mathbf{K}\frac{\partial \mathbf{D}}{\partial \rho_k} \tag{25}$$

Substituting Eq. (25) and its transposed form (assuming that **K** is symmetric) into the last two terms of Eq. (24) yields upon collection of terms, the following simple results:

$$\frac{\mathrm{d}U}{\mathrm{d}\rho_k} = -\frac{1}{2}\mathbf{D}^{\mathrm{T}}\frac{\partial \mathbf{K}}{\partial \rho_k}\mathbf{D} \tag{26}$$

Clearly from Eq. (26), for design independent loads the sensitivity of U with respect to any of the design variables ρ_k, $k = 1, \ldots, N$, can be determined as the negative of the derivative of U calculated for a fixed displacement field (see Pedersen, 1990; Olhoff et al., 1993). As the design variables ρ_k only affect the design in the local element, the expression in Eq. (26) is equivalent to

$$\frac{\partial U}{\partial \rho_k} = -\frac{1}{2}\left(\boldsymbol{d}_{\mathrm{T}}^{k}\right)\frac{\partial \boldsymbol{k}_k}{\partial \rho_k}\left(\boldsymbol{d}_k\right) \tag{27}$$

which means that the gradient vector of U for the entire structure is given by

$$\nabla U = -\frac{1}{2}\left\{\left(\boldsymbol{d}_1^{\mathrm{T}}\right)\frac{\partial \boldsymbol{k}_1}{\partial \rho_1}\left(\boldsymbol{d}_1\right), \ldots, \left(\boldsymbol{d}_k^{\mathrm{T}}\right)\frac{\partial \boldsymbol{k}_k}{\partial \rho_k}\left(\boldsymbol{d}_k\right), \ldots, \left(\boldsymbol{d}_N^{\mathrm{T}}\right)\frac{\partial \boldsymbol{k}_N}{\partial \rho_N}\left(\boldsymbol{d}_N\right)\right\}^{\mathrm{T}} \tag{28}$$

Here, the sensitivities of the local element stiffness matrices with respect to the corresponding volume densities of material can be derived analytically and Eq. (28) provides the basis for the step of sensitivity analysis of U with respect to the design variables ρ in the outer loop of the flow diagram in Fig. 4. In the next step of the outer loop, a mathematical programming routine of sequential linear programming employs the sensitivities for calculation of the optimum material distribution and in the subsequent step, the material density variables ρ are updated. The entire iterative solution procedure depicted in Fig. 4 is continued until all the iterates have converged.

6. Numerical examples and discussion

The new method and the developed software have been tested by performing a number of different full three-dimensional examples. All examples are performed using a material with Young's modulus $E = 2.10 \cdot 10^{11}$ N/m^2 and Poisson's ratio $\nu = 0.3$ unless otherwise stated, and length dimensions are given in metres. No densities above 0.99 and below 0.01 are allowed, in order to avoid numerical problems which are prone to occur if the material fractions become too small. The results are represented by grey scale, where high densities are represented by black and low densities by white.

In order to be able to visualize the three-dimensional topology designs in sufficient detail we have chosen to apply 8-node, i.e. low order, isoparametric 3D finite elements for the analyses behind all the examples presented in the following. This is due to limitations on available computer capacity; the use of higher order elements, e.g. 20-node 3D elements, is much more costly and would considerably impair a reasonably detailed visualization of the three-dimensional designs. We have checked by means of several test examples that the use of 8-node elements yields the same overall topologies as 20-node elements.

Let us now demonstrate numerically that the microstructures used in this paper provide full relaxation of the three-dimensional problems considered. As discussed in Section 1, generalized shape optimization problems often are not well-posed because the design space is not closed in the appropriate sense. A remedy to ensure closure of the set of feasible designs is to relax, i.e. regularize, the mathematical formulation of the problem by introducing composites with perforated, periodic microstructures as admissible materials for the structural design (Cheng and Olhoff, 1981, 1982; Olhoff et al., 1981; Kohn and Strang, 1982; Lurie et al., 1982a,b; Bendsøe and Kikuchi, 1988; Bendsøe, 1989). Numerical indications of the need for regularization of a given problem are lack of convergence and dependence of the designs on the size of the applied finite element mesh. In particular, if the problem is not properly regularized, it is not possible to obtain a limiting, numerically stable design by consecutively decreasing the mesh size (Cheng and Olhoff, 1981, 1982; Olhoff et al., 1981).

To illustrate the mesh independency of topologies obtained by the present method, we consider, for convenience, a planar design domain with loading and support conditions as depicted in Fig. 5a. We model the problem using 8-node 3D isoparametric finite elements as mentioned above, solve it using three different mesh sizes and obtain the solutions shown in Fig. 5b, c and d. The results clearly indicate mesh independency of the topology, and the existence of a well defined limiting design for any degree of mesh refinement. This witnesses that the applied microstructures have provided full relaxation of the problem.

It is worth noting that the solutions in Fig. 5 consist of composite in large sub-domains and that the designs in Fig. 5c and d strongly resemble that of a Mitchell truss. This is not surprising since the Mitchell truss is the optimum solution to the problem depicted in Fig. 5a provided that the amount of available material is much less than the amount prescribed in the current example.

A full three-dimensional topology optimization example is presented in Fig. 6. Here, Fig. 6a shows a cubic design domain which is subjected to four parallel concentrated loads at the upper surface and equipped with simple supports at the four corners of the lower surface. The volume fraction of available material is taken to be 0.08 relative to the design domain, and we have chosen $\nu = 0$ for the material.

Fig. 6b illustrates the optimum topology solution to this problem which is a quadropod consisting of four legs of quite distinctly solid material, each transferring one of the applied concentrated loads to the nearest simple support and a substructure made of composite material which interconnects the upper parts of the four legs.

As is clearly illustrated by the results in Fig. 5 and to a lesser extent in Fig. 6, it is a characteristic feature that the structures of optimum topology obtained by the present method generally consist of composite material in large sub-domains. There are two reasons for this. Firstly, as discussed in Section 4, depending on the state of stress, composite materials generally are much more efficient than isotropic, solid materials, and therefore largely manifest themselves in optimum solutions. Secondly, the current application of optimum microstructures as a basis for topology optimization actually prompts a larger content of composite material in the resulting solution, as compared with use of non-optimum microstructures.

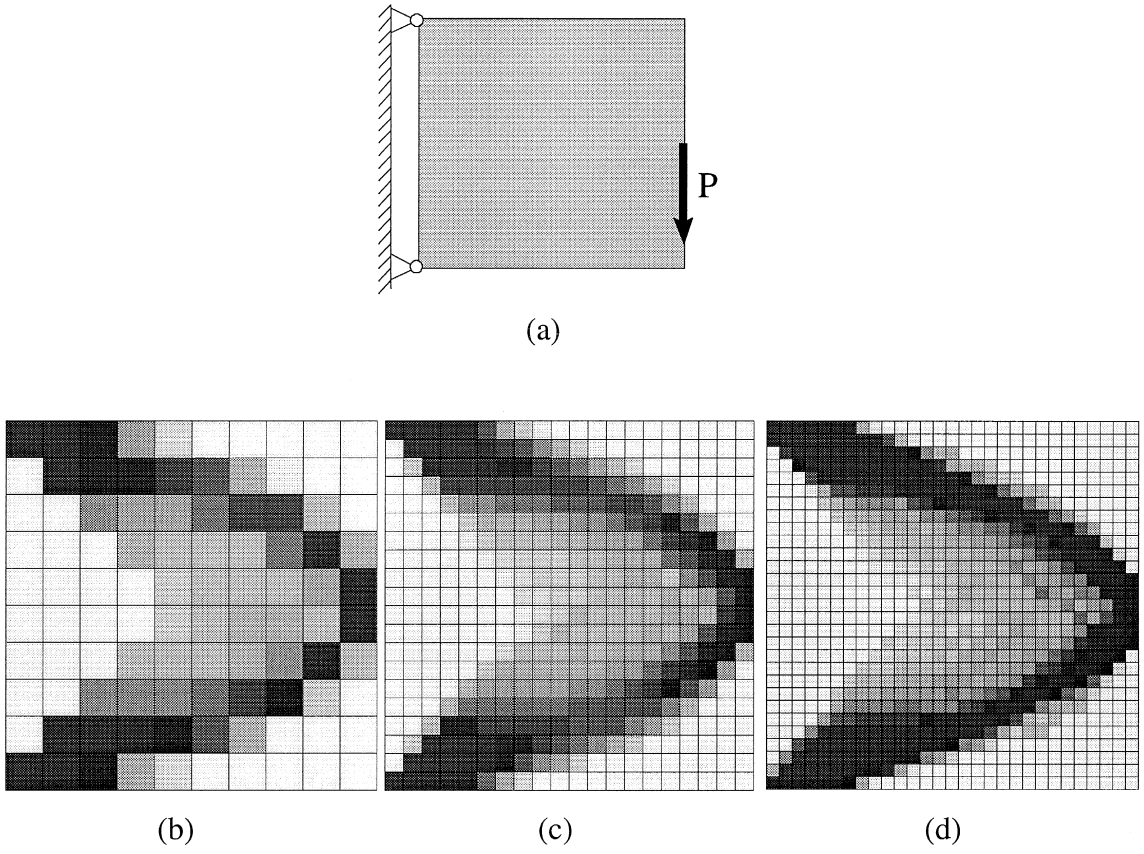

Fig. 5. Example of finite element mesh refinement. (a) Admissible design domain, loading and support conditions for the example problem. (b, c and d) Topology results obtained for different mesh sizes. It is seen that the topology is consistent.

In fact, it is the main motivation for choosing optimum microstructures as a basis for three-dimensional topology optimization in this paper that we aim at being able to determine global optimum solutions. The large structural sub-domains of composite material that are a consequence of this aim, however, often make it difficult to visualize the overall structural topology and to devise simplified sub-optimum designs that are attractive from the point of view of manufacture. To facilitate visualization, we introduce a penalization technique which reduces the amount of composite material in the solution.

We have tested different penalization techniques and chosen a commonly used method which has proven to perform satisfactorily when combined with the present method, although it can only yield 0–1 solutions for special problems. The method implies that when computing the local stiffness matrices of the finite elements, the volume density of material ρ, $0 \leq \rho \leq 1$, is raised to a power p, $p > 1$,

$$\rho_{\text{pen}} = \rho^{p}$$

which penalizes intermediate densities of material and thus makes a 0–1 solution more advantageous (see, for example, Bendsøe, 1995; Rozvany et al., 1995). The continuation approach (see Sigmund, 1994) where the optimization problem is treated unpenalized until convergence followed by a gradually increased penalization power p, is applied. The following examples are all penalized using a maximum penalization power equal to four and a penalization increment equal to one.

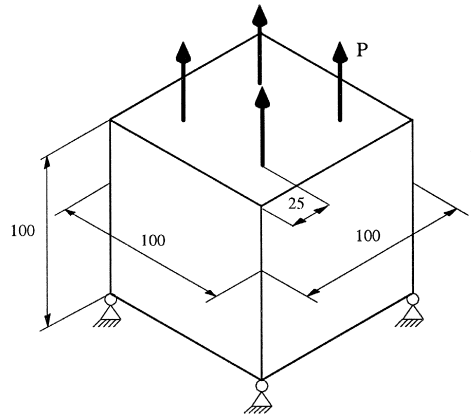

(a)

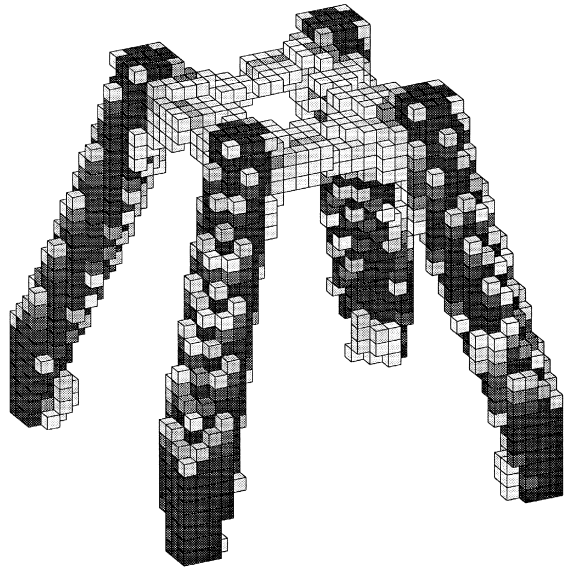

(b)

Fig. 6. Cubic design domain subjected to four point loads where $P = 10$ N. The volume fraction of available material is 0.08 and $\nu = 0$ for the material. (a) Design domain with loading and support conditions. (b) Quadropod solution to the problem with material densities less than 0.8 removed. The solution is obtained without penalization and $U_{\min} = 28.28 \cdot 10^{-10}$ N m.

It is obvious that the price for producing more distinct structural topologies by the penalization procedure is an increased value of the total elastic energy, i.e. penalized designs will be sub-optimal. However, as the application of optimum microstructures renders our topology optimization problem convex and thus ensures that we obtain the global optimum solution before penalization is carried out, we expect that the penalized solution will be in the neighborhood of the global optimum. Indeed, typical tests have shown that the increase of the value of the objective function due to penalization is less than 8%.

Fig. 7a displays an example of an oblong box-shaped design domain for which the available volume fraction of material is 0.30. The two ends of the domain are clamped and a concentrated bending moment acts at the center. Fig. 7b shows the topology solution obtained after penalization as described above, and is seen to consist

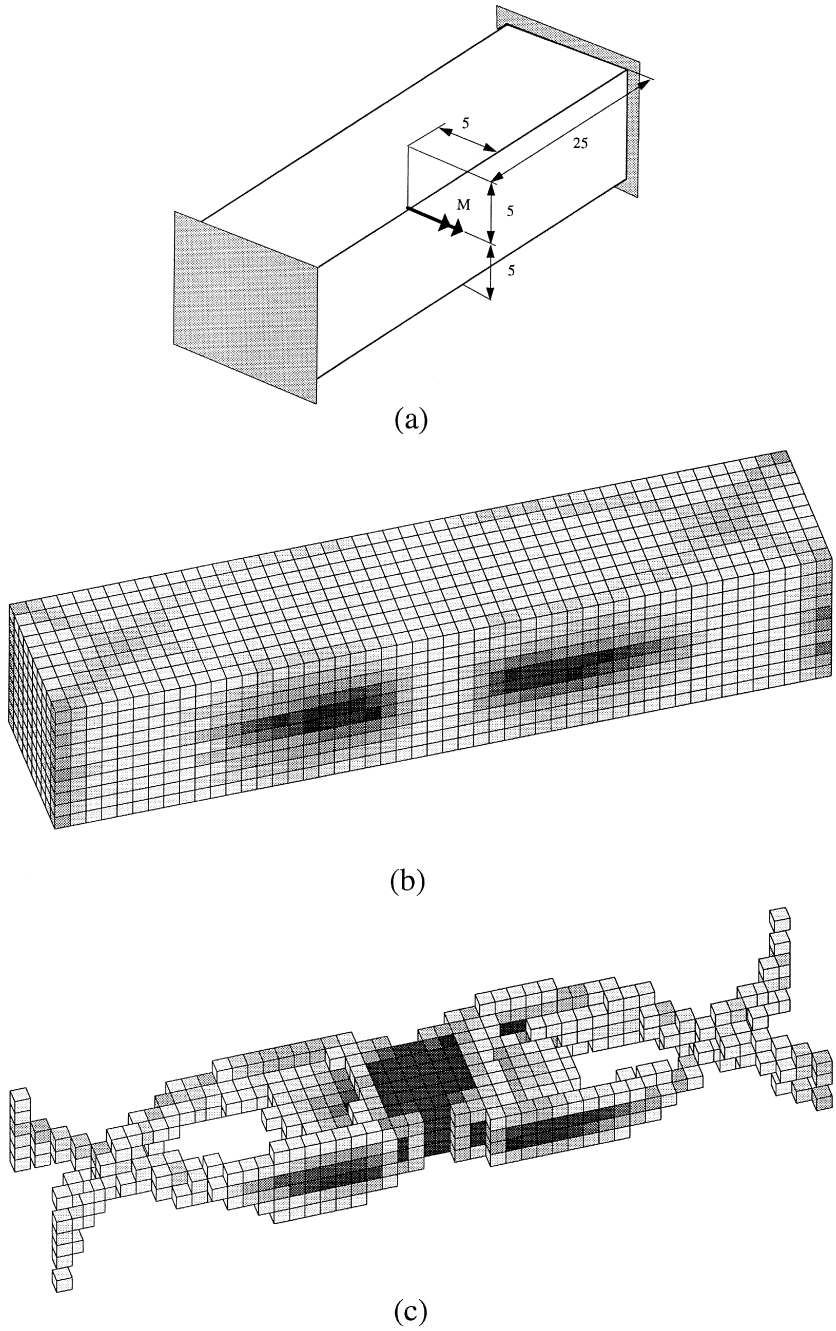

Fig. 7. Oblong box-shaped design domain with clamped ends and a concentrated bending moment acting in the center, $M = 20$ N m. The material volume fraction is 0.30. (a) Design domain with loading and support conditions. (b) Topology solution represented with all material densities present. (c) Solution depicted with densities below 0.5 removed, $U = 3.559 \cdot 10^{-10}$ N m.

still of a large part of composite material. In Fig. 7c elements with material densities below 0.5 have been removed from the solution as a means to visualize the topology.

Figs. 8 and 9 show examples of different box-shaped cantilevered design domains with different volume fractions of available material. Penalization was applied in both cases and quite distinct topologies were obtained, a truss-frame in the former example, and a tapered I-beam in the latter.

For the truss-frame, Fig. 8c presents an illustration of the principal stresses and their directions, which we recall to be of fundamental importance for the optimization of the microstructures. In Fig. 8c principal tensile

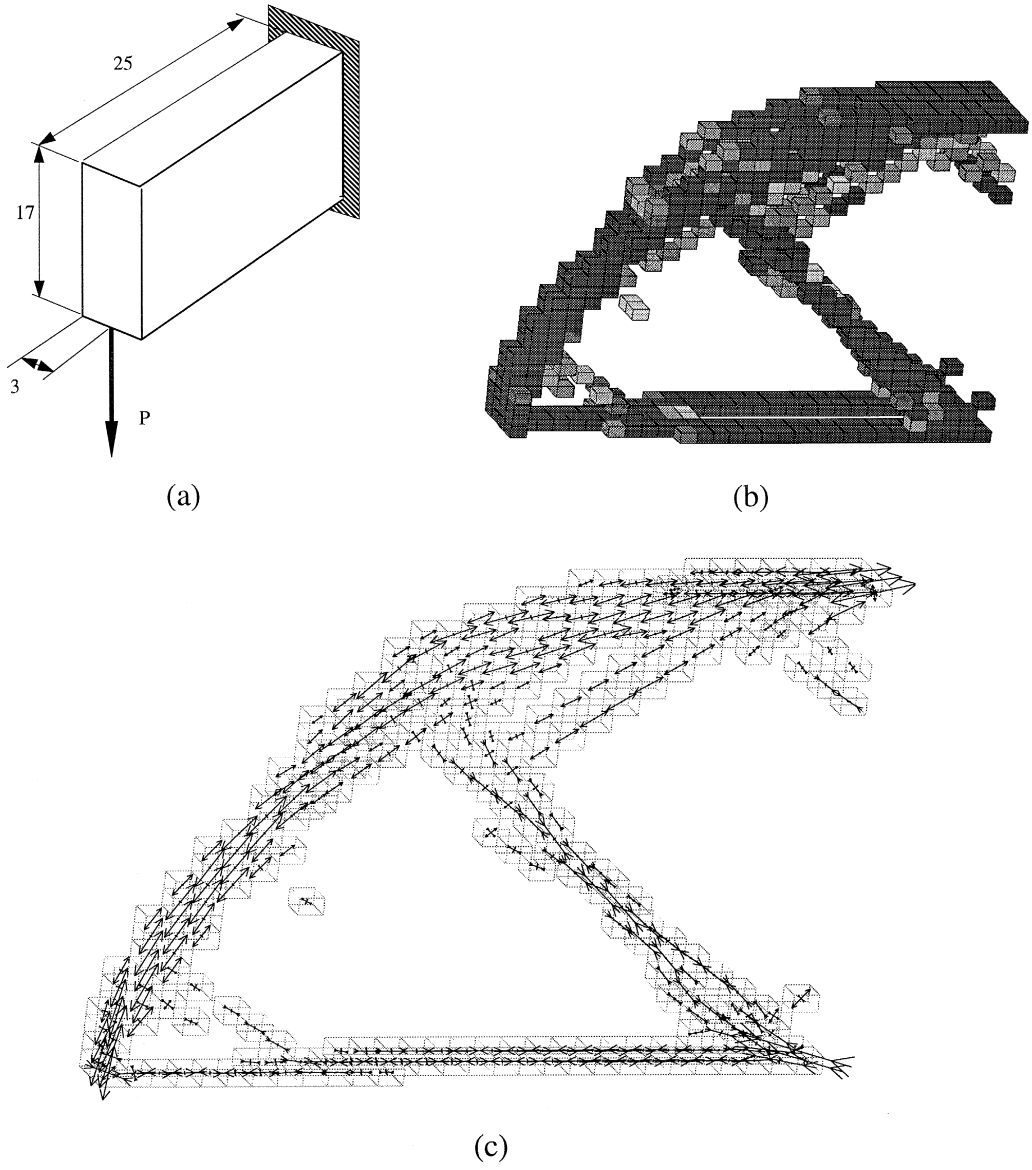

Fig. 8. Slender box-shaped cantilevered design domain subjected to a point load $P = 10$ N. The volume fraction of material is 0.3. (a) Design domain with loading and support conditions. (b) Truss-frame solution to the problem with densities less than 0.8 removed, $U = 12.029 \cdot 10^{-9}$ N m. (c) Flow of principal stresses in the truss-frame (only the half of the truss-frame which is behind the plane of symmetry is displayed).

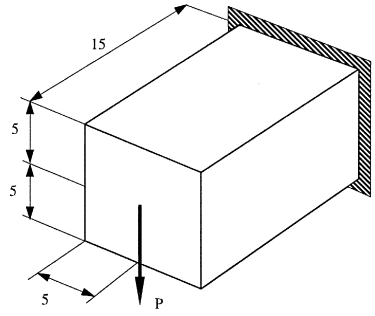

(a)

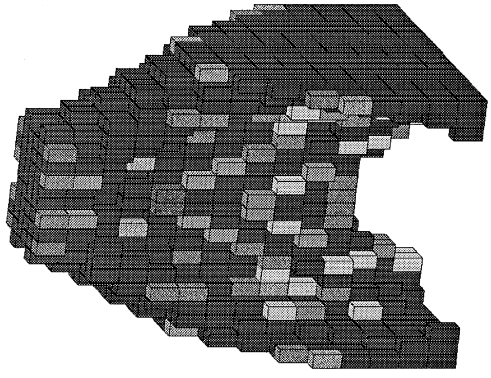

(b)

Fig. 9. Short cantilevered box-shaped design domain subjected to a point load $P = 1$ N. The volume fraction of material is 0.40. (a) Design domain with loading and support conditions. (b) Tapered I-beam solution to the problem with densities less than 0.8 removed, $U = 11.852 \cdot 10^{-11}$ N m.

stresses are indicated by $\langle$———$\rangle$ and compressive ones by $\rangle$———$\langle$ and it is interesting to note the consistency between the flow of stresses and the load, support conditions and the resulting design of the structure.

In closing this paper, authors may summarize the advantages of the current use of three-dimensional optimum microstructures for topology optimization and discuss a few alternative approaches as follows:

(i) The dependence of the effective (homogenized) macroscopic properties on the microstructure geometry is available in explicit analytic form for the material with optimum three-dimensional microstructure used in this paper.

(ii) The optimum microstructures provide a full relaxation of the three-dimensional generalized shape optimization problem. This means that the problem is well-posed and that the optimum solution is convergent with respect to finite element mesh refinement.

(iii) The use of optimum microstructures renders the topology optimization problem convex such that local solutions are avoided. This implies that a simple sensitivity based procedure of mathematical programming can be applied for solution of the complete optimization problem.

There exists a different method which disregards formation of anisotropic composite material and is a penalized material density approach based on an artificial isotropic solid material model (see, for example,

Bendsøe, 1995; Rozvany et al., 1995). In this method an artificial density-like function is adopted as the design variable, and is used to modify the stiffness matrix of a given solid material such as to make 0–1 solutions more likely. Use of the method implicitly requires that designs obtained almost entirely consist of subdomains of material and void, since there is no way to physically interpret intermediate densities. However, intermediate material densities will always appear, though sometimes only in small sub-domains. It is another weakness of the method that the material modeling does not provide regularization, and thus well-posedness, of the mathematical problem formulation, and this manifests itself by strong mesh dependency of the results.

An interesting method called the *perimeter method* has recently been presented by Haber et al. (1996) in a two-dimensional structural setting. This method does not require relaxation through introduction of anisotropic microstructures and ensures well-posedness of the generalized shape optimization problem through specification of an upper-bound constraint on the perimeter of the solid part of the structure. A generalization of this topology design method to encompass a constraint on the surface area of the solid part of a three-dimensional structure is being undertaken by Guedes (private communication) and is a very interesting alternative to the approach presented in the present paper.

Acknowledgements

Authors are indebted to Professor Andrej Cherkaev of the University of Utah, Dr. Lars A. Krog of Aalborg University for many fruitful discussions and to Dr. Erik Lund of Aalborg University for aid in computer implementation of the developments in this paper. The research received partial support from the Danish Technical Research Council (Programme of Research on Computer Aided Design) and from the Faculty of Technology and Science of Aalborg University.

References

Allaire, G., 1994. Explicit lamination parameters for three-dimensional shape optimization. Control Cybernetics 23, 311–326.

Allaire, G., Bonnetier, E., Francfort, G., Jouve, F., 1996. Shape optimization by the homogenization method. Report. Lab. d'Analyse Numerique, Universite Paris 6, France, 43 pp.

Bendsøe, M.P., 1989. Optimal shape design as a material distribution problem. Struct. Opt. 1, 193–202.

Bendsøe, M.P., 1995. Optimization of Structural Topology, Shape and Material. Springer-Verlag, Berlin.

Bendsøe, M.P., Kikuchi, N., 1988. Generating optimal topologies in structural design using a homogenization method. Comput. Math. Appl. Mech. Eng. 71, 197–224.

Cheng, K.-T., Olhoff, N., 1981. An investigation concerning optimal design of solid elastic plates. Int. J. Solids Struct. 17, 305–323.

Cheng, K.-T., Olhoff, N., 1982. Regularized formulation for optimal design of axisymmetric plates. Int. J. Solids Struct. 18, 153–169.

Cherkaev, A.V., Palais, R., 1996. Optimal design of three-dimensional axisymmetric elastic structures. Struct. Opt. 12, 35–45.

Gibiansky, L.V., Cherkaev, A.V., 1987. Microstructures of composites of extremal rigidity and exact estimates of provided energy density (in Russian). Report No. 1155. A.F. Ioffe Physical-Technical Institute, Academy of Sciences of the USSR, Leningrad. English translation in: Kohn, R.V., Cherkaev, A.V. (Eds.), Topics in the Mathematical Modelling of Composite Materials. Birkhaüser, New York. 1997.

Haber, R.B., Jog, C.S., Bendsøe, M.P., 1996. A new approach to variable-topology shape design using a constraint on perimeter. Struct. Opt. 11, 1–12.

Kohn, R.V., Strang, G., 1982. Structural design optimization, homogenization and regularization of vibrational problems. In: Lecture Notes in Physics, vol. 154. Springer, Berlin, pp. 131–147.

Lurie, K.A., Cherkaev, A.V., Fedorov, A.V., 1982a. Regularization of optimal design problems for bars and plates. JOTA 37 (1), 499–522.

Lurie, K.A., Cherkaev, A.V., Fedorov, A.V., 1982b. Regularization of optimal design problems for bars and plates. JOTA 37 (2), 523–543.

Olhoff, N., Lurie, K.A., Cherkaev, A.V., Fedorov, A.V., 1981. Sliding regimes and anisotropy in optimal design of vibrating axisymmetric plates. Int. J. Solids Struct. 17, 931–948.

Olhoff, N., Bendsøe, M.P., Rasmussen, J., 1991. On CAD-integrated structural topology and design optimization. Comput. Math. Appl. Mech. Eng. 89, 259–279.

Olhoff, N., Thomsen, J., Rasmussen, J., 1992. Topology optimization of bi-material structures. In: Pedersen, P. (ed.), Proc. IUTAM Symp. Optimal Design with Advanced Materials, 18–20 August, Lyngby, Denmark. Springer-Verlag, Berlin, pp. 191–206.

Pedersen, P., 1990. Bounds on elastic energy in solids of orthotropic materials. Struct. Opt. 2, 55–63.

Rozvany, G.I.N., Bendsøe, M.P., Kirsch, U., 1995. Layout optimization of structures. Appl. Mech. Rev. 48 (2).

Sigmund, O., 1994. Design of material structures using topology optimization. Ph.D. Thesis. DCAMM Report S 69. Technical University of Denmark.